J|A|C|S
ARTICLES
Published on Web 05/11/2002

In Search of Covalently Bound Tetra- and Penta-Oxygen Species: A Photoelectron Spectroscopic and Ab Initio Investigation of MO_4^- and MO_5^- (M = Li, Na, K, Cs)

Hua-Jin Zhai,[†] Xin Yang,[†] Xue-Bin Wang,[†] Lai-Sheng Wang,*[,†] Ben Elliott,[‡] and Alexander I. Boldyrev*[,‡]

Contribution from the Department of Physics, Washington State University, 2710 University Drive, Richland, Washington 99352, W. R. Wiley Environmental Molecular Sciences Laboratory, Pacific Northwest National Laboratory, MS K8-88, P.O. Box 999, Richland, Washington 99352, and Department of Chemistry and Biochemistry, Utah State University, Logan, Utah 84322-0300

Abstract: Although neutral and ionic $O_4^{0/-/+}$ species have been observed experimentally and considered for energetic materials, O_4^{2-} and O_5^{2-} dianions have not yet been explored. O_4^{2-} is valent isoelectronic to the well-known ClO_3^- and SO_3^{2-} anions, and O_5^{2-} is valent isoelectronic to ClO_4^- and SO_4^{2-}. All are stable, common anions in solutions and inorganic salts. In this article, we explore the possibility of making covalently bound O_4^{2-} and O_5^{2-} species stabilized in the forms of $M^+O_4^{2-}$ and $M^+O_5^{2-}$ (M = Li, Na, K, Cs) in the gas phase. Laser vaporization experiments using M-containing targets and an O_2-seeded carrier gas yielded very intense mass peaks corresponding to MO_4^- and MO_5^-. To elucidate the structure and bonding of the newly observed MO_4^- and MO_5^- species, we measured their photoelectron spectra and then compared them with ab initio calculations and the spectra of ClO_3^-, $Na^+SO_3^{2-}$, ClO_4^-, and $Na^+SO_4^{2-}$. Careful analyses of the experimental and ab initio results showed, however, that the observed species are of the forms, $O_2^-M^+O_2^-$ and $O_2^-M^+O_3^-$. The more interesting $M^+O_4^{2-}$ and $M^+O_5^{2-}$ species were found to be higher-energy isomers, but they are true minima on the potential energy surfaces, which suggests that it might be possible to synthesize bulk materials containing covalently bound tetra- and pentatomic oxygen building blocks.

Introduction

Among all chemicals, oxygen (O_2) plays the most important role in life on the Earth. Although O_2 was discovered more than two hundred years ago by Lavoisier and helped start the chemistry revolution, our knowledge about higher oxygen molecules beyond molecular oxygen (O_2) and ozone (O_3) is very limited. The $(O_2)_2$ dimer was known as early as 1885 as a collision complex of ground-state oxygen molecules,[1] giving broad and diffuse atmospheric absorption bands. The first spectroscopic investigation of $(O_2)_2$ was carried out by Long and Ewing,[2] who recorded the low-resolution gas-phase spectrum of the 578-nm band. Since then, studies of van der Waals complexes of O_2 have enjoyed a long history of investigations [see refs 4−11 and references therein]. The van der Waals dimer, $(O_2)_2$, has a very weak binding energy of 0.01 eV.[2] Adamantidies et al.[3] theoretically predicted the covalently bound cyclic (D_{2h}) form of O_4. This stimulated considerable further theoretical effort, because this cyclic O_4, ∼5.3 eV higher in energy than two separate O_2 molecules, appeared to be a promising candidate as a high-energy-density material.[4−8] Subsequent theoretical studies have also identified a D_{3h} form analogous to SO_3 at a somewhat higher energy, 6.5 eV.[9,10] None of these covalent O_4 structures has yet been experimentally observed.[11]

Over the past 25 years[12−21], a large number of matrix isolation works have been devoted to $M^+O_4^-$ (M = Na, K, Rb, Cs) molecules and the isolated O_4^- anion. On the basis of good agreement between B3LYP/6-311+G* calculations and ob-

* E-mails: ls.wang@pnl.gov or boldyrev@cc.usu.edu.
[†] Washington State University and Pacific Northwest National Laboratory.
[‡] Utah State University.

(1) Janssen, J. *CR Acad. Sci.* **1885**, *101*, 349.
(2) Long, C. A.; Ewing, G. E. *J. Chem. Phys.* **1973**, *58*, 4824.
(3) Adamantidies, V.; Neisius, D.; Verhaegen, G. *Chem. Phys.* **1980**, *48*, 215.
(4) Campargue, A.; Biennier, L.; Kachanov, A.; Jost, R.; Bussery-Honvault, B.; Veyret, V.; Churassy, S.; Bacis, R. *Chem. Phys. Lett.* **1988**, *288*, 734.
(5) Aquilanti, V.; Ascenzi, D.; Bartolomei, M.; Cappelletti, D.; Cavalli, S.; de Castro Vitores, M.; Pirani, F. *Phys. Rev. Lett.* **1999**, *82*, 69.
(6) Peterka, D. S.; Ahmed, M.; Suits, A. G.; Wilson, K. J.; Korkin, A.; Nooijen, M.; Bartlett, R. J. *J. Chem. Phys.* **1999**, *110*, 6095.
(7) Seidl, E. T.; Schaefer, H. F. *J. Chem. Phys.* **1988**, *88*, 7043; **1992**, *96*, 1176.
(8) Dunn, K. M.; Scuseria, G. E.; Schaefer, H. F. *J. Chem. Phys.* **1990**, *92*, 6077.
(9) Roeggen, I.; Nilssen, E. W. *Chem. Phys. Lett.* **1989**, *157*, 409.
(10) Hottoka, M.; Pyykko, P. *Chem. Phys. Lett.* **1989**, *157*, 415.
(11) Cacace, F.; de Petris, G.; Troiani, A. *Angew. Chem., Int. Ed.* **2001**, *40*, 4062.
(12) Andrews, L. *J. Chem. Phys.* **1971**, *54*, 4935.
(13) Jacox, M. E.; Milligan, D. E. *Chem. Phys. Lett.* **1972**, *14*, 518.
(14) Andrews, L.; Hwang, J. T.; Trindle, C. *J. Phys. Chem.* **1973**, *77*, 1065.
(15) Smardzewski, R. R.; Andrews, L. *J. Chem. Phys.* **1972**, *57*, 1327; *J. Phys. Chem.* **1973**, *77*, 801.
(16) Andrews, L. *J. Mol. Spectrosc.* **1976**, *61*, 337.
(17) Lindsay, D. M.; Herschbach, D. R.; Kwiram, A. L. *J. Phys. Chem.* **1983**, *87*, 2113.
(18) Han, C. C.; Johnson, M. A. *Chem. Phys. Lett.* **1992**, *189*, 460. DeLuca, M. J.; Han, C. C.; Johnson, M. A. *J. Chem. Phys.* **1990**, *93*, 268.
(19) Manceron, L.; Le Quere, A. M.; Perchard, J. P. *J. Phys. Chem.* **1989**, *93*, 2960.
(20) Thompson, M.; Jacox, M. E. *J. Chem. Phys.* **1989**, *91*, 3826.
(21) Chertihin, G. V.; Andrews, L. *J. Chem. Phys.* **1998**, *108*, 6404.

10.1021/ja020097k CCC: $22.00

served infrared spectra of the O_4^- anion in Ar matrixes, Chertichin and Andrews concluded that O_4^- has a rectangular structure with two short O−O distances (1.267 Å) and two long O−O distances (2.073 Å).[21] Such an anion was found in gas-phase mass spectrometric studies,[22,23] and its photoelectron spectra have been reported by Hanold and Continetti.[24] The O_4^- anion was found to be stable with respect to $O_2 + O_2^-$ by about 0.46 eV.[23] Aquino, Taylor, and Walch have performed the most accurate ab initio calculations on O_4^- using the CASSCF-ICCI level of theory and aug-cc-pVTZ basis sets.[25] Their results agree well with the infrared spectra of O_4^- in Ar matrixes[21] and the photodissociation and photodetachment data.[24]

The O_4^{2-} and O_5^{2-} dianions, however, have not yet been studied as potential candidates for oxygen-rich materials. O_4^{2-} is valent isoelectronic to ClO_3^- and SO_3^{2-}, and O_5^{2-} is valent isoelectronic to ClO_4^- and SO_4^{2-}, which are all well-known anions in solutions and inorganic salts. Hence, it might be possible to stabilize the analogous O_4^{2-} and O_5^{2-} dianions and make them as part of an inorganic salt. In this article, we explore the possibility of producing a covalently bound tetraoxide and pentaoxide in the forms of MO_4^- and MO_5^- (M = Li, Na, K, Cs) in the gas phase. Abundant MO_4^- and MO_5^- were produced using laser vaporization of alkali-containing targets and an O_2-seeded carrier gas. The structure and bonding of these newly observed species were investigated by combining photodetachment photoelectron spectroscopy (PES) and ab initio calculations. PES of size-selected anions combined with a laser vaporization cluster source has been proven to be a powerful experimental technique to study the electronic structure of a wide range of novel molecular and cluster species.[26−28] To further test our results, we also investigated ClO_3^-, ClO_4^-, $NaSO_3^-$, and $NaSO_4^-$ and compared their PES data to ab initio results.

Experimental Methods

The experiments were performed using two magnetic-bottle PES apparatuses, one equipped with a laser vaporization supersonic cluster source[29] and the other with an electrospray ion source.[30] The MO_4^- and MO_5^- (M = Li, Na, K, and Cs) experiments were preformed with the laser vaporization PES apparatus. The MO_4^- and MO_5^- anions were generated by laser vaporization of a M_2CO_3 (M = Li, Na, K, and Cs) target with a helium carrier gas seeded with 0.5% O_2. Silver powder was used as a binder in order to compress the M_2CO_3 powder into hardened targets under relatively low pressure. Clusters formed from the laser vaporization source were entrained in the He carrier gas and underwent a supersonic expansion. The anion species in the beam were extracted perpendicularly into a time-of-flight (TOF) mass spectrometer. The MO_4^- and MO_5^- species were selected and decelerated before photodetachment by a 193-nm laser beam from an ArF excimer laser. Photoelectron TOF spectra were obtained and converted to electron binding energy spectra calibrated by the known spectrum of Rh^-. The instrumental resolution of the laser vaporization apparatus was $\sim\Delta E/E \sim 2.5\%$, that is, ~25 meV for 1 eV kinetic energy electrons at full ion deceleration. However, because of the low photodetachment cross sections of the cluster species studied herein, full ion deceleration was not feasible, and all of the obtained spectra have lower resolution than the intrinsic instrumental resolution.

The PES spectrum of $NaSO_3^-$ was measured using the electrospray apparatus.[30] Briefly, a 10^{-4} M Na_2SO_3 salt solution was sprayed at ambient conditions through a 0.01-mm-diameter needle biased at −2.2 kV. The resulting negatively charged droplets were fed into a 3-cm-long, 0.5-mm-i.d. desolvation capillary and heated to ~50 °C. Anionic species emerged from the desolvation capillary and were guided by a radio frequency quadrupole system into a quadrupole ion trap. The anions were accumulated in the ion trap for 0.1 s before being pushed into the extraction zone of a TOF mass spectrometer. For the PES experiment, both 193- and 157-nm photons from an excimer laser were used for photodetachment. The PES spectra were calibrated by the known spectra of I^- and O^-. The energy resolution of the electrospray apparatus was ~11 meV at 0.4 eV kinetic energy but deteriorated significantly at 193 or 157 nm as a result of the laser bandwidth and the strong background present at these wavelengths.

Computational Methods

We first optimized the geometries of ClO_x^- and $NaSO_x^-$ ($x = 3, 4$), and MO_4^- and MO_5^- (M = Li, Na, K), employing analytical gradients with polarized split-valence basis sets (6-311+G*)[31−33] with a hybrid method that includes a mixture of Hartree−Fock exchange with density functional exchange-correlation (B3LYP).[34−36] The lowest energy structures thereby identified were refined at the MP2(full)[37] and CCSD(T)[38−40] levels of theory. Finally, the energies of the lowest structures were refined further using the CCSD(T) level of theory and 6-311+G(2df) basis sets.

Vertical electron detachment energies (VDEs) from the lowest-energy structures of ClO_3^-, $NaSO_3^-$, LiO_4^-, and NaO_4^- were calculated using the restricted or unrestricted outer valence Green function (UOVGF) method[41−45] incorporated in Gaussian-98. For some lowest states, we also calculated VDEs using the CCSD/6-311+G(2df) and CCSD(T)/6-311+G(2df) levels of theory. The UOVGF calculations assured that we did not miss any one-electron detachment processes, because they allow us to calculate VDEs from all orbitals (except the singlet excited states). The core electrons were kept frozen in treating the electron correlation at the UOVGF, CCSD, and CCSD(T) levels of theory. All calculations were performed using the Gaussian-98 program.[46]

Experimental Results

Mass Spectra for MO_4^- and MO_5^- (M = Li and Na). Typical mass spectra for LiO_4^-/LiO_5^- and NaO_4^-/NaO_5^- from

(22) Conway, D. C.; Nesbit, L. E. *J. Chem. Phys.* **1968**, *48*, 509.
(23) Hiroaka, K. *J. Chem. Phys.* **1988**, *89*, 3190.
(24) Hanold, K. A.; Continetti, R. E. *Chem. Phys.* **1998**, *239*, 493. Hanold, K. A.; Garner, M. C.; Continetti, R. E. *Phys. Rev. Lett.* **1996**, *77*, 3335.
(25) Aquino, A. J. A.; Taylor, P. R.; Walch, S. P. *J. Chem. Phys.* **2001**, *114*, 3010.
(26) Li, X.; Wang, L. S.; Boldyrev, A. I.; Simons, J. *J. Am Chem. Soc.* **1999**, *121*, 6033.
(27) Li, X.; Kuznetsov, A. E.; Zhang, H. F.; Boldyrev, A. I.; Wang, L. S. *Science* **2001**, *291*, 859.
(28) Boldyrev, A. I.; Wang, L. S. *J. Phys. Chem. A* **2001**, *105*, 10759.
(29) Wang, L. S.; Cheng, H. S.; Fan, J. *J. Chem. Phys.* **1995**, *102*, 9480. Wang, L. S.; Wu, H. In *Advances in Metal and Semiconductor Clusters. IV. Cluster Materials*; Duncan, M. A, Ed.; JAI Press: Greenwich, 1998, pp 299−343.
(30) Wang, L. S.; Ding, C. F.; Wang, X. B.; Barlow, S. E. *Rev. Sci. Instrum.* **2000**, *70*, 1957.
(31) McLean, D.; Chandler, G. S. *J. Chem. Phys.* **1980**, *72*, 5639.
(32) Clark, T.; Chandrasekhar, J.; Spitznagel, G. W.; Schleyer, P. v. R. *J. Comput. Chem.* **1983**, *4*, 294.
(33) Frisch, M. J.; Pople, J. A.; Binkley, J. S. *J. Chem. Phys.* **1984**, *80*, 3265.
(34) Parr, R. G.; Yang, W. *Density-Functional Theory of Atoms and Molecules*: Oxford University Press: Oxford, 1989.
(35) Becke, A. D. *J. Chem. Phys.* **1992**, *96*, 2155.
(36) Perdew, J. P.; Chevary, J. A.; Vosko, S. H.; Jackson, K. A.; Pederson, M. R.; Singh, D. J.; Fiolhais, C. *Phys. Rev. B* **1992**, *46*, 6671.
(37) Krishnan, R.; Binkley, J. S.; Seeger, R.; Pople, J. A. *J. Chem. Phys.* **1980**, *72*, 650.
(38) Cizek, J. *Adv. Chem. Phys.* **1969**, *14*, 35.
(39) Purvis, G. D., III; Bartlett, R. J. *J. Chem. Phys.* **1982**, *76*, 1910.
(40) Scuseria, G. E.; Janssen, C. L.; Schaefer, H. F., III. *J. Chem. Phys.* **1988**, *89*, 7282.
(41) Cederbaum, L. S. *J. Phys. B* **1975**, *8*, 290.
(42) von Niessen, W.; Shirmer, J.; Cederbaum, L. S. *Comput. Phys. Rep.* **1984**, *1*, 57.
(43) Zakrzewski, V. G.; von Niessen, W. *J. Comput. Chem.* **1993**, *14*, 13.
(44) Zakrzewski, V. G.; Ortiz, J. V. *Int. J. Quantum Chem.* **1995**, *53*, 583.
(45) Ortiz, J. V.; Zakrzewski, V. G.; Dolgunitcheva, O. In *Conceptual Trends in Quantum Chemistry*; Kryachko, E. S., Ed.; Kluwer, Dordrecht, 1997; Vol 3, p 463.

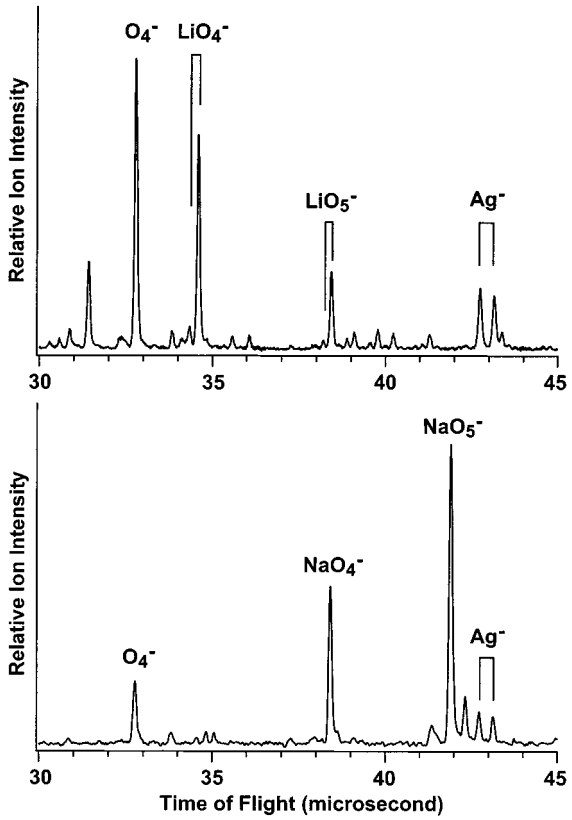

Figure 1. Typical anion mass spectra of MO_x^- species (M = Li, Na) from the laser vaporization of composite M_2CO_3/Ag targets using O_2-seeded helium carrier gas.

the laser vaporization supersonic cluster source are shown in Figure 1. Abundant MO_4^- and MO_5^- mass signals wereobserved, along with much weaker signals for MO_3^- and almost no signals for MO^- and MO_2^-. Strong O_4^- mass signals were also observed. Our mass resolution ($M/\Delta M$ = 400) was sufficient for definitive assignments of the observed anions. All of the four alkali systems showed similar mass patterns, except that the NaO_5^- signal was the strongest among the MO_5^- species.

The dominance of the MO_4^- and MO_5^- species and the absence of the MO^-, MO_2^-, or MO_3^- anions in the current experiment were surprising. In our previous experimental study of CuO_x^- species,[47] for example, we abundantly found all anionic oxides for $x = 1-6$. The present observation initially led us to suspect that perhaps in the presence of alkali ions, covalently bound large ionic oxygen clusters, such as O_4^{2-} and O_5^{2-}, might have been formed. Such doubly charged anions were seemingly possible, analogous to the well-known valence isoelectronic species SO_3^{2-} and ClO_3^-, and SO_4^{2-} and ClO_4^-, respectively. To address this possibility and characterize the

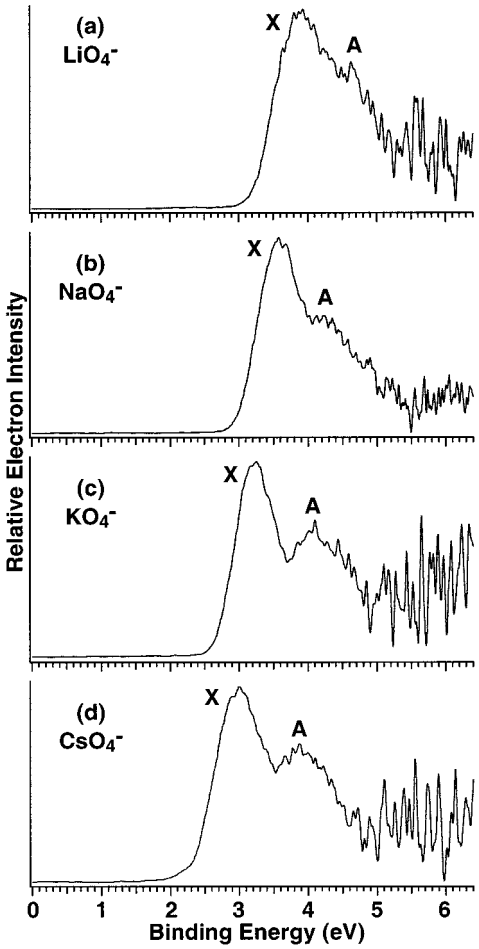

Figure 2. Photoelectron spectra of MO_4^- (M = Li, Na, K, Cs) at 193 nm (6.424 eV).

observed MO_4^- and MO_5^- species, we performed a combined PES and ab initio investigation.

Photoelectron Spectra of MO_4^- (M = Li, Na, K, Cs). Figure 2 shows the PES spectra of MO_4^- (M = Li, Na, K, Cs) at 193 nm. Despite the strong MO_4^- mass signals, all of these species appeared to have rather low photodetachment cross sections, which presents quite a challenge for measuring the PES spectra. In addition, strong background electrons were present at 193 nm, as shown at the high-binding-energy side of all of the spectra. The PES spectra for the four species were similar, each with two very broad bands (*X* and *A*) that became more separated for the heavier species. The spectral similarity suggested that these species are likely to have similar structures. The electron binding energies gradually decrease as the alkali atom gets heavier, indicating that the electron affinities (EAs) of neutral MO_4 decrease from M = Li to Cs. Since no vibrational structures were resolved in the PES spectra, the adiabatic detachment energies (ADEs) were evaluated by drawing a straight line along the leading edge of the *X* band and adding a constant to the intersection with the binding energy axis to take into account the instrumental resolution. The measured ADEs and VDEs for the four MO_4^- species are given in Table 1. Because of the broad spectral features, large uncertainties were assessed for the obtained binding energies.

Photoelectron Spectrum of NaO_5^-. Figure 3 shows the PES spectrum of NaO_5^- at 193 nm. Four well-separated detachment bands, labeled *X*, *A*, *B*, and *C*, were revealed. Similar PES

(46) Frisch, M. J.; Trucks, G. M.; Schlegel, H. B.; Scuseria, G. E.; Robb, M. A.; Cheeseman, J. R.; Zakrzewski, V. G.; Montgomery, J. A., Jr.; Stratmann, R. E.; Burant, J. C.; Dapprich, S.; Millam, J. M.; Daniels, A. D.; Kudin, K. N.; Strain, M. C.; Farkas, O.; Tomasi, J.; Barone, V.; Cossi, M.; Cammi, R.; Mennucci, B.; Pomelli, C.; Adamo, C.; Clifford, S.; Ochterski, J.; Petersson, G. A.; Ayala, P. Y.; Cui, Q.; Morokuma, K.; Malick, D. K.; Rabuck, A. D.; Raghavachari, K.; Foresman, J. B.; Cioslowski, J.; Ortiz, J. V.; Baboul, A. G.; Stefanov, B. B.; Liu, G.; Liashenko, A.; Piskorz, P.; Komaromi, I.; Gomperts, R.; Martin, R. L.; Fox, D. J.; Keith, T.; Al-Laham, M. A.; Peng, C. Y.; Nanayakkara, A.; Gonzales, C.; Challacombe, M.; Gill, P. M. W.; Johnson, B. G.; Chen, W.; Wong, M. W.; Andres, J. L.; Head-Gordon, M.; Replogle, E. S.; Pople, J. A. *Gaussian 98*, revision A.7. Gaussian, Inc.: Pittsburgh, PA, 1998.
(47) Wu, H.; Desai, S. R.; Wang, L. S. *J. Phys. Chem. A* **1997**, *101*, 2103.

Table 1. Observed Adiabatic (ADE) and Vertical (VDE) Detachment Energies for LiO_4^-, NaO_4^-, KO_4^-, CsO_4^-, NaO_5^-, and $NaSO_3^-$ in eV[a]

	ADE	VDE
	LiO_4^-	
X	3.3 (0.2)	3.90 (0.10)
A		4.6 (0.1)
	NaO_4^-	
X	3.1 (0.2)	3.60 (0.10)
A		4.2 (0.1)
	KO_4^-	
X	2.8 (0.2)	3.21 (0.08)
A		4.1 (0.1)
	CsO_4^-	
X	2.5 (0.2)	2.96 (0.08)
A		3.9 (0.1)
	NaO_5^-	
X	3.2 (0.2)	3.53 (0.08)
A		4.55 (0.06)
B		5.75 (0.04)
C		6.15 (0.10)
	$NaSO_3^-$	
X	2.3 (0.2)	2.72 (0.10)
A		3.01 (0.10)
B		4.20 (0.10)
C		5.52 (0.08)

[a] The numbers in the parentheses represent the experimental uncertainty.

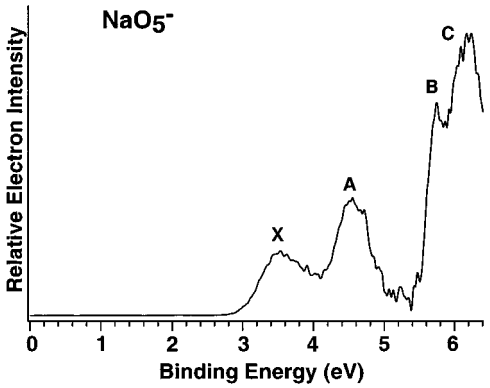

Figure 3. Photoelectron spectra of NaO_5^- at 193 nm.

spectral features were also recorded for other MO_5^- (M = Li, K, and Cs) species but were not shown, because they were of poor quality as a result of weak anion signals and low photodetachment cross sections. Similarly to the MO_4^- series, we also observed that the binding energies of the MO_5^- species decrease from M = Li to Cs. The observed ADE and VDEs for NaO_5^- are also given in Table 1.

Photoelectron Spectrum of $NaSO_3^-$. Figure 4 shows the PES spectrum of $NaSO_3^-$ at 157 nm with three well-resolved bands. The lowest binding-energy band appeared to contain two features (*X* and *A*). The *B* and *C* bands were well-separated. We also obtained the PES spectrum of $NaSO_3^-$ at 193 nm (not shown) and obtained identical spectral features. The ADE and VDEs for all the spectral features of $NaSO_3^-$ are also listed in Table 1.

Theoretical Results

Structures of ClO_3^- and ClO_4^-. We optimized the geometry of ClO_3^- ($^1A_1$, $1a_1^2 1e^4 2a_1^2 3a_1^2 2e^4 3e^4 4e^4 1a_2^2 4a_1^2$) with C_{3v} symmetry and that of ClO_4^- ($^1A_1$, $1a_1^2 1t_2^6 2a_1^2 2t_2^6 1e^4 3t_2^6 4e^4$-

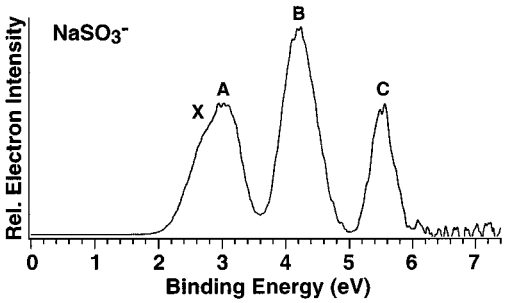

Figure 4. Photoelectron spectrum of $NaSO_3^-$ at 157 nm (7.866 eV).

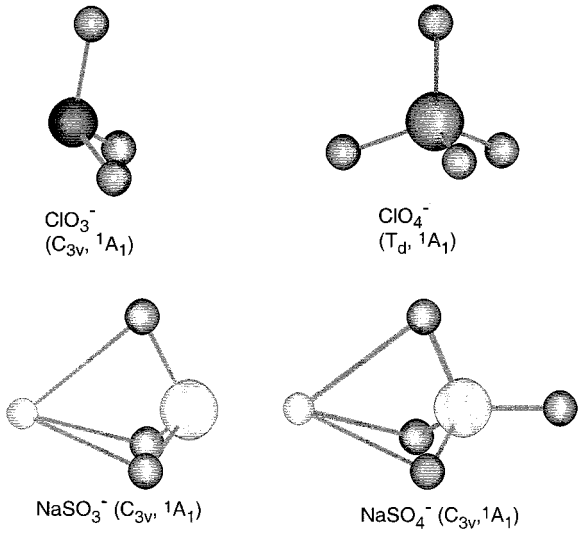

Figure 5. Structures of ClO_3^-, ClO_4^-, $NaSO_3^-$, and $NaSO_4^-$.

Table 2. Calculated Molecular Parameters of ClO_3^- and ClO_4^-

	theory		
	B3LYP/6-311+G*	CCSD(T)/6-311+G*	condensed phase data[a]
ClO_3^-, C_{3v}, $^1A_1$			
R(Cl−O), Å	1.542	1.536	1.48−1.57
∠OClO, deg	108.5	108.4	107−108
E_t, au	−685.76711	−684.68945	
$\omega_1(a_1)$, cm^{-1}	830		939
$\omega_2(a_1)$, cm^{-1}	528		614
$\omega_3(e)$, cm^{-1}	864		971
$\omega_4(e)$, cm^{-1}	410		489
ClO_4^-, T_d, $^1A_1$			
R(Cl−O), Å	1.500	1.492	1.35−1.53
E_t, au	−760.93252	−759.69498	
$\omega_1(a_1)$, cm^{-1}	805		928
$\omega_2(e)$, cm^{-1}	397		459
$\omega_3(t_2)$, cm^{-1}	970		1119
$\omega_4(t_2)$, cm^{-1}	555		625

[a] The structural data are from ref 48 and the vibrational data are from ref 49.

$1t_1^6$) with T_d symmetry (Figure 5) using B3LYP/6-311+G* and CCSD(T)/6-311+G* levels of theory. We also calculated harmonic frequencies for both anions at the B3LYP/6-311+G* level of theory. Our optimized parameters and harmonic frequencies are presented in Table 2 along with the available crystal data. Our results are in good agreement with the crystal data.[48,49] We believe these results can be used as references in evaluating the new experimental and ab initio results.

(48) Solymosi, F. *Structure and Stability of Salts of Halogen Oxyacids in Solid Phase*; John Wiley & Sons: London, 1977.
(49) Nakamoto, K. *Infrared and Raman Spectra of Inorganic and Coordination Compounds*, Part A, 5th ed.; John Wiley & Sons: New York, 1997.

Table 3. Calculated Molecular Properties of the Most Stable $NaSO_3^-$ and $NaSO_4^-$ Structures

$NaSO_3^-$ (C_{3v}, $^1A_1$) B3LYP/6-311+G*	$NaSO_3^-$ (C_{3v}, $^1A_1$) CCSD(T)/6-311+G*	SO_3^{2-} (C_{3v}, $^1A_1$) condensed phase data[a]	$NaSO_4^-$ (C_{3v}, $^1A_1$) B3LYP/6-311+G*	SO_4^{2-} (T_d, $^1A_1$) condensed phase data[a]
R(S−O) = 1.573 Å	R(S−O) = 1.571 Å	R(S−O) = 1.51 Å	R(S−O_b) = 1.539 Å[b] R(S−O_t) = 1.479 Å[c]	R(S−O) = 1.49 Å
∠OSO = 103.6°	∠OSO = 103.5°	∠OSO = 106°	∠O_bSO_b = 105.3° [b]	∠OSO = 109.5°
R(Na−S) = 2.483 Å	R(Na−S) = 2.506 Å		R(Na−S) = 2.459 Å	
E_t = −786.326 57 au	E_t = −784.843 16 au		E_t = −861.573 59 au	
$\omega_1(a_1)$ = 857 cm^{-1}		$\omega_1(a_1)$ = 967 cm^{-1}	$\omega_1(a_1)$ = 1161 cm^{-1}	$\omega_1(a_1)$ = 983 cm^{-1}
$\omega_2(a_1)$ = 607 cm^{-1}		$\omega_2(a_1)$ = 620 cm^{-1}	$\omega_2(a_1)$ = 865 cm^{-1}	$\omega_3(t_2)$ = 1105 cm^{-1}
$\omega_3(a_1)$ = 347 cm^{-1}			$\omega_3(a_1)$ = 597 cm^{-1}	$\omega_4(t_2)$ = 611 cm^{-1}
$\omega_4(e)$ = 850 cm^{-1}		$\omega_3(e)$ = 933 cm^{-1}	$\omega_4(a_1)$ = 356 cm^{-1}	
$\omega_5(e)$ = 455 cm^{-1}		$\omega_4(e)$ = 469 cm^{-1}	$\omega_5(e)$ = 949 cm^{-1}	$\omega_3(t_2)$ = 1105 cm^{-1}
$\omega_6(e)$ = 181 cm^{-1}			$\omega_6(e)$ = 559 cm^{-1}	$\omega_4(t_2)$ = 611 cm^{-1}
			$\omega_7(e)$= 415 cm^{-1}	$\omega_2(e)$ = 450 cm^{-1}
			$\omega_8(e)$ =143 cm^{-1}	

[a] The structural data are from ref 48 and the vibrational frequencies are from ref 49. [b] *b* means bridged oxygen. [c] *t* means terminal oxygen.

Table 4. Calculated Molecular Properties for the Isomers of LiO_4^-, NaO_4^-, and KO_4^- [a,b]

B3LYP/6-311+G*	CCSD(T)/6-311+G*	B3LYP/6-311+G*	CCSD(T)/6-311+G*	B3LYP/6-311+G*	CCSD(T)/6-311+G*
LiO_4^- (C_{3v}, $^1A_1$)	LiO_4^- (C_{3v}, $^1A_1$)	NaO_4^- (C_{3v}, $^1A_1$)	NaO_4^- (C_{3v}, $^1A_1$)	KO_4^- (C_{3v}, $^1A_1$)	KO_4^- (C_{3v}, $^1A_1$)
R(Li−O_c) = 1.861 Å	R(Li−O_c) = 1.881 Å	R(Na−O_c) = 2.258 Å	R(Na−O_c) = 2.368 Å	R(K−O_c) = 2.526 Å	R(K−O_c) = 2.593 Å
R(O_c−O_b) = 1.474 Å	R(O_c−O_b) = 1.481 Å	R(O_c−O_b) = 1.462 Å	R(O_c−O_b) = 1.498 Å	R(O_c−O_b) = 1.463 Å	R(O_c−O_b) = 1.471 Å
∠O_b−O_c−O_b = 106.3°	∠O_b−O_c−O_b = 105.9°	∠O_b−O_c−O_b = 108.5°	∠O_b−O_c−O_b = 107.8°	∠O_b−O_c−O_b = 109.2°	∠O_b−O_c−O_b = 108.8°
E_t = −308.32770 au	E_t = −307.59822 au	E_t = −463.07450 au	E_t = −461.95998 au	E_t = −900.70910 au	E_t = −899.44463 au
$\omega_1(a_1)$ = 830 cm^{-1}		$\omega_1(a_1)$ = 782 cm^{-1}		$\omega_1(a_1)$ = 771 cm^{-1}	
$\omega_2(a_1)$ = 659 cm^{-1}		$\omega_2(a_1)$ = 619 cm^{-1}		$\omega_2(a_1)$ = 590 cm^{-1}	
$\omega_3(a_1)$ = 593 cm^{-1}		$\omega_3(a_1)$ = 365 cm^{-1}		$\omega_3(a_1)$ = 294 cm^{-1}	
$\omega_4(e)$ = 631 cm^{-1}		$\omega_4(e)$ = 641 cm^{-1}		$\omega_4(e)$ = 639 cm^{-1}	
$\omega_5(e)$ = 497 cm^{-1}		$\omega_5(e)$ = 468 cm^{-1}		$\omega_5(e)$ = 442 cm^{-1}	
$\omega_6(e)$ = 327 cm^{-1}		$\omega_6(e)$ = 246 cm^{-1}		$\omega_6(e)$ = 214 cm^{-1}	
LiO_4^- (D_{2d}, $^3B_2$)	LiO_4^- (D_{2d}, $^3B_2$)	NaO_4^- (D_{2d}, $^3B_2$)	NaO_4^- (D_{2d}, $^3B_2$)	KO_4^- (D_{2d}, $^3B_2$)	KO_4^- (D_{2d}, $^3B_2$)
R(Li−O) = 1.899 Å	R(Li−O) = 1.899 Å	R(Na−O) = 2.263 Å	R(Na−O) = 2.361 Å	R(K−O) = 2.594 Å	R(K−O) = 2.600 Å
R(O−O) = 1.347 Å	R(O−O) = 1.357 Å	R(O−O) = 1.349 Å	R(O−O) = 1.376 Å	R(O−O) = 1.344 Å	R(O−O) = 1.353 Å
∠O−Li−O = 41.5°	∠O−Li−O = 41.9°	∠O−Na−O = 34.7°	∠O−Na−O = 33.9°	∠O−K−O = 30.0°	∠O−K−O = 30.2°
E_t = −308.443 81 au	E_t = −307.710 02 au	E_t = −463.191 17 au	E_t = −462.072 76 au	E_t = −900.826 50 au	E_t = −899.554 96 au
$\omega_1(a_1)$ = 1166 cm^{-1}		$\omega_1(a_1)$ = 1161 cm^{-1}		$\omega_1(a_1)$ = 1168 cm^{-1}	
$\omega_2(a_1)$ = 247 cm^{-1}		$\omega_2(a_1)$ = 218 cm^{-1}		$\omega_2(a_1)$ = 193 cm^{-1}	
$\omega_3(b_1)$ = 74 cm^{-1}		$\omega_3(b_1)$ =33 cm^{-1}		$\omega_3(b_1)$ = 31 cm^{-1}	
$\omega_4(b_2)$ = 1168 cm^{-1}		$\omega_4(b_2)$ = 1161 cm^{-1}		$\omega_4(b_2)$ = 1168 cm^{-1}	
$\omega_5(b_2)$ = 714 cm^{-1}		$\omega_5(b_2)$ = 398 cm^{-1}		$\omega_5(b_2)$ = 281 cm^{-1}	
$\omega_6(e)$ = 370 cm^{-1}		$\omega_6(e)$ = 258 cm^{-1}		$\omega_6(e)$ = 244 cm^{-1}	
$\omega_7(e)$ = 166 cm^{-1}		$\omega_7(e)$ = 98 cm^{-1}		$\omega_7(e)$ = 54 cm^{-1}	

[a] *c* means central oxygen. [b] *b* means bridged oxygen.

Structures of $NaSO_3^-$ and $NaSO_4^-$. We optimized the geometry of $NaSO_3^-$ with a pyramidal C_{3v} symmetry ($^1A_1$, $1a_1^2$-$1e^4 2a_1^2 3a_1^2 2e^4 3e^4 4e^4 1a_2^2 4a_1^2$), as shown in Figure 5, using B3LYP/6-311+G* and CCSD(T)/6-311+G* levels of theory. Optimized geometrical parameters are presented in Table 3. The bonding between Na^+ and SO_3^{2-} is mainly ionic; thus, our calculated results for the SO_3^{2-} dianion in $NaSO_3^-$ can be compared to the corresponding crystal data (Table 3).[48,49] A satisfactory agreement was observed for both the geometrical parameters and the harmonic frequencies.

We have previously investigated $NaSO_4^-$ experimentally and theoretically and found two stable minima for this ion pair, $Na^+SO_4^{2-}$.[50] The lowest energy geometry at the B3LYP/tzvp+ level of theory was found to be C_{3v} symmetry, as shown in Figure 5. Single-point energies were computed for both symmetries at the CCSD(T)/6-311+G* level of theory, and the C_{3v} symmetry was shown to be more stable by 0.82 kcal/mol. In the present study, we reoptimized the geometry of $NaSO_4^-$ with a C_{3v} symmetry using the B3LYP/6-311+G* level of theory and found very similar geometrical parameters. Our optimized geometrical parameters are presented in Table 3. Calculated S−O bond lengths (1.479 and 1.573 Å) for the SO_4^{2-} dianion in $Na^+SO_4^{2-}$ are very close to the corresponding crystal data (1.49 Å). The computed vibrational frequencies also agree with experiment values.[49]

Structures of MO_4^- (M = Li, Na, K). For the new oxygen-containing species, we first optimized the geometries and calculated harmonic frequencies of LiO_4^-, NaO_4^-, and KO_4^- with structures containing a covalently bound O_4^{2-} dianion under C_{3v} symmetry ($^1A_1$, $1a_1^2 1e^4 2a_1^2 3a_1^2 2e^4 3e^4 4e^4 1a_2^2 4a_1^2$) at the B3LYP/6-311+G* levels of theory. Optimized geometrical parameters and frequencies are presented in Table 4. We found that the C_{3v} covalently bound LiO_4^-, NaO_4^-, and KO_4^- are all true minima (Figure 6). We then reoptimized the geometries of LiO_4^- and NaO_4^- at the CCSD(T)/6-311+G* level of theory and found a very good agreement at the two levels of theory (Table 4). We tested the applicability of the one-electron approximation for the C_{3v} structures of MO_4^- by running CASSCF(12,11)/6-311+G* calculations (106 953 configurations). We found that the Hartree−Fock configuration is dominant (its coefficient in the CASSCF expansion, C_{HF}, is 0.999), thus showing reliability of our CCSD(T)/6-311+G*

(50) Wang, X. B.; Ding, C. F.; Nicholas, J. B.; Dixon, D. A.; Wang, L. S. *J. Phys. Chem. A* **1999**, *103*, 3423.

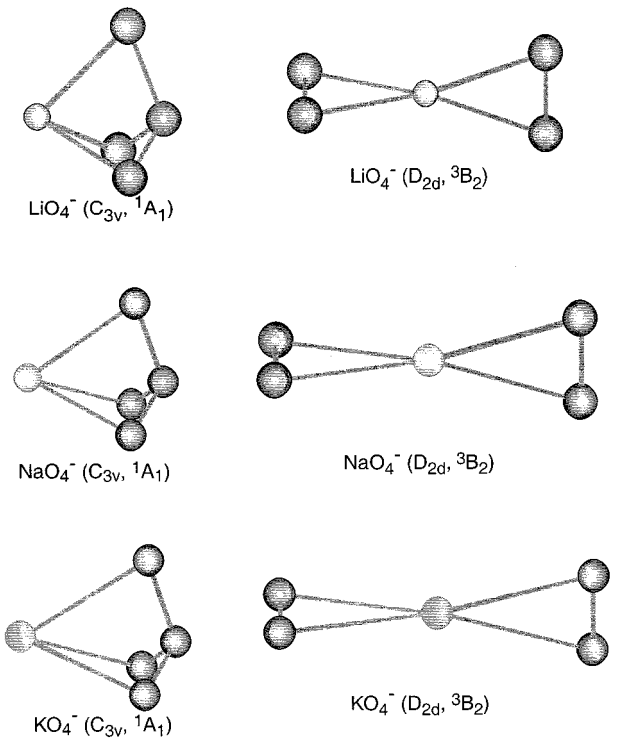

Figure 6. Structures of MO_4^- (M = Li, Na, K) with C_{3v} and D_{2d} symmetries.

calculations. The geometrical parameters of the pyramidal C_{3v} O_4^{2-} dianion were found to be reasonable when compared to the isoelectronic and isostructural SO_3^{2-} in $NaSO_3^-$, suggesting that chemical species containing an O_4^{2-} dianion may be viable. Of course, such compounds, if made, would be highly energetic materials.

However, we found that the most stable structures of MO_4^- (M = Li, Na, K) have a D_{2d} symmetry ($^3B_2$, $1a_1^2 1b_2^2 1e^4 2e^4 2a_1^2 2b_2^2 3b_2^2 3a_1^2 3e^4 1b_1^1 1a_2^1$) with two separate O_2^- units located on opposite sides of a central cation M^+ ($O_2^- M^+ O_2^-$), as shown in Figure 6. Optimized geometrical parameters for this structure are also given in Table 4. Again, we tested the applicability of the one-electron approximation for the D_{2d} structures of MO_4^- by running CASSCF(10,12)/6-311+G* calculations (313 236 configurations). We found that the Hartree−Fock configuration was dominant (C_{HF} = 0.978), thus showing reliability of our CCSD(T)/6-311+G* calculations. The energies of the C_{3v} structures relative to the global minimum structures were calculated to be 2.41 (LiO_4^-), 2.95 (NaO_4^-), and 2.90 eV (KO_4^-) [all at CCSD(T)/6-311+G(2df) level].

Structures of MO_5^- (M = Li, Na, K). We first optimized the geometries and calculated at the B3LYP/6-311+G* level of theory harmonic frequencies of LiO_5^-, NaO_5^-, and KO_5^- using structures containing a covalently bound O_5^{2-} dianion with a C_{3v} symmetry ($^1A_1$, $1a_1^2 1e^4 2a_1^2 3a_1^2 2e^4 3e^4 4e^4 1a_2^2 4a_1^2$). Optimized geometrical parameters are presented in Table 5. All three species were found to have a true local minimum at the covalently bound C_{3v} structure, as shown in Figure 7. The tetrahedral structure of the O_5^{2-} dianion is perturbed substantially in the C_{3v} MO_5^- species with the bond length difference between $R(O_c-O_b)$ and $R(O_c-O_t)$ being 0.24 (LiO_5^-), 0.22 (NaO_5^-), and 0.19 Å (KO_5^-), all at B3LYP/6-311+G* (see Table 5). We tested the applicability of the one-electron approximation for the C_{3v} structures of MO_5^- by running

Table 5. Calculated Molecular Properties for the Isomers of LiO_5^-, NaO_5^-, and KO_5^- [a,b,c]

B3LYP/6-311+G*	B3LYP/6-311+G*	B3LYP/6-311+G*
LiO_5^- (C_{3v}, $^1A_1$)	NaO_5^- (C_{3v}, $^1A_1$)	KO_5^- (C_{3v}, $^1A_1$)
$R(Li-O_c)$ = 1.950 Å	$R(Na-O_c)$ = 2.316 Å	$R(K-O_c)$ = 2.663 Å
$R(O_c-O_b)$ = 1.547 Å	$R(O_c-O_b)$ = 1.541 Å	$R(O_c-O_b)$ = 1.527 Å
$R(O_c-O_t)$ = 1.307 Å	$R(O_c-O_t)$ = 1.319 Å	$R(O_c-O_t)$ = 1.335 Å
$\angle O_b-O_c-O_t$ = 115.3°	$\angle O_b-O_c-O_t$ = 113.1°	$\angle O_b-O_c-O_t$ = 112.5°
E_t = −383.414 12 au	E_t = −538.162 11 au	E_t = −975.797 32 au
$\omega_1(a_1)$ = 900 cm^{-1}	$\omega_1(a_1)$ = 853 cm^{-1}	$\omega_1(a_1)$ = 798 cm^{-1}
$\omega_2(a_1)$ = 662 cm^{-1}	$\omega_2(a_1)$ = 591 cm^{-1}	$\omega_2(a_1)$ = 600 cm^{-1}
$\omega_3(a_1)$ = 573 cm^{-1}	$\omega_3(a_1)$ = 487 cm^{-1}	$\omega_3(a_1)$ = 450 cm^{-1}
$\omega_4(a_1)$ = 444 cm^{-1}	$\omega_4(a_1)$ = 317 cm^{-1}	$\omega_4(a_1)$ = 268 cm^{-1}
$\omega_5(e)$ = 694 cm^{-1}	$\omega_5(e)$ = 675 cm^{-1}	$\omega_5(e)$ = 675 cm^{-1}
$\omega_6(e)$ = 456 cm^{-1}	$\omega_6(e)$ = 418 cm^{-1}	$\omega_6(e)$ = 400 cm^{-1}
$\omega_7(e)$ = 333 cm^{-1}	$\omega_7(e)$ = 326 cm^{-1}	$\omega_7(e)$ = 342 cm^{-1}
$\omega_8(e)$ = 279 cm^{-1}	$\omega_8(e)$ = 218 cm^{-1}	$\omega_8(e)$ = 182 cm^{-1}
LiO_5^- (C_{2v}, $^3B_2$)	NaO_5^- (C_{2v}, $^3B_2$)	KO_5^- (C_{2v}, $^3B_2$)
$R(Li-O_{b1})$ = 1.888 Å	$R(Na-O_{b1})$ = 2.263 Å	$R(K-O_{b1})$ = 2.583 Å
$R(Li-O_{b2})$ = 2.016 Å	$R(Na-O_{b2})$ = 2.341 Å	$R(K-O_{b2})$ = 2.711 Å
$R(O_{b1}-O_{b1})$ = 1.345 Å	$R(O_{b1}-O_{b1})$ = 1.349 Å	$R(O_{b1}-O_{b1})$ = 1.344 Å
$R(O_c-O_{b2})$ = 1.352 Å	$R(O_c-O_{b2})$ = 1.351 Å	$R(O_c-O_{b2})$ = 1.351 Å
$\angle O_{b2}-O_c-O_{b2}$ = 112.2°	$\angle O_{b2}-O_c-O_{b2}$ = 113.8°	$\angle O_{b2}-O_c-O_{b2}$ = 114.6°
E_t = −383.623 70 au	E_t = −538.376 59 au	E_t = −976.009 66 au
$\omega_1(a_1)$ = 1163 cm^{-1}	$\omega_1(a_1)$ = 1159 cm^{-1}	$\omega_1(a_1)$ = 1169 cm^{-1}
$\omega_2(a_1)$ = 1063 cm^{-1}	$\omega_2(a_1)$ = 1064 cm^{-1}	$\omega_2(a_1)$ = 1063 cm^{-1}
$\omega_3(a_1)$ = 662 cm^{-1}	$\omega_3(a_1)$ = 639 cm^{-1}	$\omega_3(a_1)$ = 617 cm^{-1}
$\omega_4(a_1)$ = 640 cm^{-1}	$\omega_4(a_1)$ = 365 cm^{-1}	$\omega_4(a_1)$ = 265 cm^{-1}
$\omega_5(a_1)$ = 196 cm^{-1}	$\omega_5(a_1)$ = 178 cm^{-1}	$\omega_5(a_1)$ = 152 cm^{-1}
$\omega_6(a_2)$ = 65 cm^{-1}	$\omega_6(a_2)$ = 34 cm^{-1}	$\omega_6(a_2)$ = 25 cm^{-1}
$\omega_7(b_1)$ = 394 cm^{-1}	$\omega_7(b_1)$ = 259 cm^{-1}	$\omega_7(b_1)$ = 248 cm^{-1}
$\omega_8(b_1)$ = 221 cm^{-1}	$\omega_8(b_1)$ = 160 cm^{-1}	$\omega_8(b_1)$ = 90 cm^{-1}
$\omega_9(b_1)$ = 112 cm^{-1}	$\omega_9(b_1)$ = 80 cm^{-1}	$\omega_9(b_1)$ = 46 cm^{-1}
$\omega_{10}(b_2)$ = 893 cm^{-1}	$\omega_{10}(b_2)$ = 883 cm^{-1}	$\omega_{10}(b_2)$ = 876 cm^{-1}
$\omega_{11}(b_2)$ = 297 cm^{-1}	$\omega_{11}(b_2)$ = 210 cm^{-1}	$\omega_{11}(b_2)$ = 165 cm^{-1}
$\omega_{12}(b_2)$ = 124 cm^{-1}	$\omega_{12}(b_2)$ = 84 cm^{-1}	$\omega_{12}(b_2)$ = 50 cm^{-1}

[a] *c* means central oxygen. [b] *b* means bridged oxygen. [c] *t* means terminal oxygen.

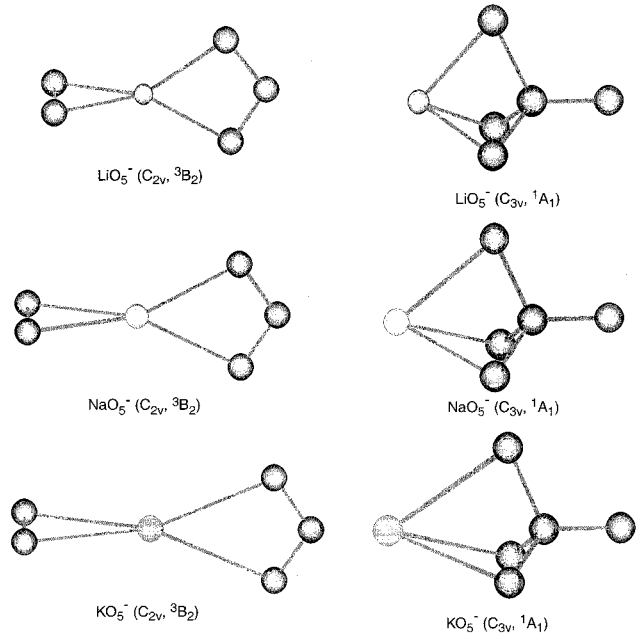

Figure 7. Structures of MO_5^- (M = Li, Na, K) with C_{2v} and C_{3v} symmetries.

CASSCF(12,11)/6-311+G* calculations (106 953 configurations) and found that the Hartree−Fock configuration is dominant (C_{HF} = 0.999).

Again, the global minimum for the MO_5^- species was found to have two separate O_2^- and O_3^- units interacting with an M^+ electrostatically (C_{2v} symmetry $O_2^- M^+ O_3^-$), as also shown in Figure 7. The structural parameters for this structure are also

Table 6. Calculated Electron Detachment Processes and Vertical Detachment Energies (VDE) for the C_{3v} ($^1A_1$) Pyramidal Structure of ClO_3^- As Compared with the Experimental VDE

			theory, VDE (eV)	
	exptl[a] VDE (eV)	final state	OVGF/6-311+G(2df)[b]	CCSD(T)/6-311+G(2df)[c]
		ClO_3^-		
X	4.65 ± 0.10	...$3e^4 4e^4 1a_2^2 4a_1^1$	4.64 (0.91)	4.52 [4.68]
		...$3e^4 4e^4 1a_2^1 4a_1^2$	5.13 (0.90)	4.70 [4.91]
A	5.75 ± 0.15	...$3e^4 4e^3 1a_2^2 4a_1^2$	6.14 (0.90)	
B	7.1 ± 0.01	...$3e^3 4e^4 1a_2^2 4a_1^2$	7.24 (0.90)	
		ClO_4^-		
X	5.50 ± 0.10	...$2t_2^6 1e^4 3t_2^6 1t_1^5$	5.89 (0.90)	5.60 [5.93]
		...$2t_2^6 1e^4 3t_2^5 1t_1^6$	7.88 (0.90)	
		...$2t_2^6 1e^3 3t_2^6 1t_1^6$	8.50 (0.90)	

[a] From ref 51. [b] Pole strength is given in parentheses. [c] VDE calculated at CCSD/6-311+G(2df) is given in brackets.

Table 7. Calculated Electron Detachment Processes and Vertical Detachment Energies (VDE) for the C_{3v} ($^1A_1$) Structures of $NaSO_3^-$ and $NaSO_4^-$ as Compared with the Experimental VDE

			theory, VDE (eV)	
anion peak	exptl[a] VDE (eV)	final state	OVGF/6-311+G(2df)[b]	CCSD(T)/6-311+G(2df)[c]
		$NaSO_3^-$		
X	2.72 ± 0.10	...$3e^4 4e^4 1a_2^2 4a_1^1$	3.00 (0.91)	2.88 [2.93]
A	3.01 ± 0.10	...$3e^4 4e^4 1a_2^1 4a_1^2$	3.68 (0.91)	3.09 [3.22]
B	4.20 ± 0.10	...$3e^4 4e^3 1a_2^2 4a_1^2$	4.66 (0.91)	
C	5.52 ± 0.08	...$3e^3 4e^4 1a_2^2 4a_1^2$	6.00 (0.91)	
		$NaSO_4^-$		
X	~3.8	...$5a_1^2 4e^4 5e^4 1a_2^1$	4.20 (0.91)	3.92 [4.09]
	~4.1	...$5a_1^2 4e^4 5e^3 1a_2^2$	4.51 (0.91)	
A	5.84 ± 0.05	...$5a_1^2 4e^3 5e^4 1a_2^2$	6.09 (0.91)	
		...$5a_1^1 4e^4 5e^4 1a_2^2$	6.74 (0.91)	

[a] VDEs for $NaSO_4^-$ are from ref 50. [b] Pole strength is given in parentheses. [c] VDE calculated at CCSD/6-311+G(2df) is given in brackets.

given in Table 5. We tested the applicability of the one-electron approximation for the C_{2v} structures of MO_5^- by running CASSCF(12,11)/6-311+G* calculations (106 941 configurations), and again we found that the Hartree−Fock configuration is dominant ($C_{HF} = 0.999$). We found that the C_{2v} structures are more stable than the covalently bound C_{3v} structures by 5.7 (LiO_5^-), 5.8 (NaO_5^-), and 5.8 eV (KO_5^-) (all at the B3LYP/6-311+G* level). Since all of the C_{3v} MO_5^- species are true minima, they are viable targets for chemical syntheses and would also be extremely energetic materials.

Spectral Assignments and Discussion

We first compare ab initio and experimental photoelectron spectra for the ClO_3^- and ClO_4^- anions, which are well-known, and the interpretation is expected to be straightforward. Then we will discuss theoretical and experimental results on $NaSO_3^-$ and $NaSO_4^-$ before proceeding with the assignment and interpretation of the experimental spectra on MO_4^- and MO_5^-, which are the main focus of the current study.

Photoelectron Spectra of ClO_3^- and ClO_4^-. We reported previously the photoelectron spectra of ClO_3^- and ClO_4^-.[51] In the present study, we calculated their VDEs at the OVGF/6-311+G(2df), CCSD/6-311+G(2df), and CCSD(T)/6-311+G(2df) levels for both anions and compared them with the experimental results in Table 6. We found good agreement for the first VDE for both anions. It should be pointed out that the VDEs at CCSD and CCSD(T) agree with each other within 0.3 eV, showing that perturbation evaluation of triple excitations in CCSD(T) is justified. Agreement is also satisfactory for the other detachment channels of ClO_3^-. According to the OVGF and CCSD(T) results, the peak marked X should consist of two one-electron transitions,[51] from HOMO ($4a_1$) and HOMO-1 ($1a_2$). The broad width of the peak X is consistent with this assignment. The second (A) and third (B) peaks in the spectrum should correspond to detachment from the two doubly degenerate 4e and 3e MOs, respectively, according to the OVGF results. Both the A and B peaks were very broad, likely due to the Jahn−Teller effect expected for detaching electrons from the degenerate MOs.

Photoelectron Spectra of $NaSO_3^-$ and $NaSO_4^-$. Photoelectron spectra of $NaSO_4^-$ have been studied previously by us,[50] but the photoelectron spectra of $NaSO_3^-$ have not yet been reported. We calculated the VDEs of both anions at the OVGF/6-311+G(2df) and CCSD(T)/6-311+G(2df) levels. In Table 7, we compare our theoretical VDEs with the current experimental results for $NaSO_3^-$ and the previous experimental results for $NaSO_4^-$. We observed reasonable agreement between the theoretical and experimental VDEs for both anions. According to the OVGF and CCSD(T) results, the peak X in the spectra of $NaSO_4^-$ (ref 50) should consist of two one-electron transitions, from HOMO ($4a_1$) and HOMO-1 (4e), according to the OVGF results.

Photoelectron Spectra of LiO_4^-, NaO_4^-, KO_4^-, and CsO_4^-. The main theme of the current study was to use the photoelectron spectra of MO_4^- (M = Li, Na, K, Cs) in conjunction with theoretical calculations to verify if the experimentally observed species actually contain the covalently bound O_4^{2-} dianion. First, we note that whereas the spectral patterns of ClO_3^- and $NaSO_3^-$ exhibit some similarity, the PES spectra of MO_4^- are very different from those of the valent isoelectronic ClO_3^- and $NaSO_3^-$, hinting that their structures might be different. The PES spectra for all of the MO_4^- species (Figure 2) are very broad, suggesting large geometry changes between the anions and the neutral states. In fact, the broad spectra of the MO_4^- species are more consistent with the dissociative detachment processes, as was observed by Hanold and Continetti for the photodetachment of bare O_4^-.[24]

To obtain more insight into the structure and bonding of MO_4^-, we calculated their photoelectron spectra for both the C_{3v} and the D_{2d} structures using the OVGF method and the extended 6-311+G(2df) basis sets. The theoretical results are compared with experimental data in Table 8 for the C_{3v} and D_{2d} structures. Surprisingly, the calculated first VDEs for both structures are in good agreement with the experimental data. The major differences were for higher-energy-detachment channels. Overall, our ab initio results for the D_{2d} $O_2^-M^+O_2^-$ structure agree better with the experimental data. Hence, we believe that the gas-phase MO_4^- species observed in our experiments should be due to the D_{2d} $O_2^-M^+O_2^-$ species instead of the covalently bound $M^+O_4^{2-}$ species that we were pursuing. This conclusion is also consistent with the energetics of the two isomers. According to our calculations, the $O_2^-M^+O_2^-$ isomer was found to be more stable than the $M^+O_4^{2-}$ isomer by ~2.4−2.9 eV.

An additional hint that the observed species were the $O_2^-M^+O_2^-$ came from the diffuseness of the experimental PES spectra. As we mentioned above, the spectra were rather broad with poorly resolved features and low detachment cross sections,

(51) Wang, X. B.; Wang, L. S. *J. Chem. Phys.* **2000**, *113*, 10928.

Table 8. Calculated Electron Detachment Processes and Vertical Detachment Energies (VDE) for the D_{2d} ($^3B_2$) and C_{3v} ($^1A_1$) Structures of LiO_4^-, NaO_4^-, and KO_4^- As Compared with the Experimental VDE[a]

anion peak	exptl VDE	final state[b] (D_{2d})	theory[c] VDE(D_{2d}) OVGF/ 6-311+G(2df)	final state (C_{3v})	theory[c] VDE(C_{3v}) OVGF/ 6-311+G(2df)
			LiO_4^-		
X	3.90 ± 0.10	$...2e^43e^31b_1^11a_2^1$	3.87 (0.93)	$...3e^44e^44a_1^21a_2^1$	3.85 (0.90)
A	4.6 ± 0.1	$...2e^43e^41b_1^11a_2^0$	4.88 (0.90)	$...3e^44e^44a_1^11a_2^2$	4.38 (0.89)
		$...2e^43e^41b_1^01a_2^1$	4.94 (0.90)	$...3e^44e^34a_1^21a_2^2$	4.71 (0.90)
		$...2e^33e^41b_1^11a_2^1$	7.44 (0.93)	$...3e^34e^44a_1^21a_2^2$	5.85 (0.89)
			NaO_4^-		
X	3.60 ± 0.10	$...2e^43e^31b_1^11a_2^1$	3.55 (0.93)	$...3e^44e^44a_1^21a_2^1$	3.32 (0.89)
A	4.2 ± 0.1	$...2e^43e^41b_1^11a_2^0$	4.77 (0.90)	$...3e^44e^44a_1^11a_2^2$	3.65 (0.90)
		$...2e^43e^41b_1^01a_2^1$	4.78 (0.90)	$...3e^44e^34a_1^21a_2^2$	4.06 (0.90)
		$...2e^33e^41b_1^11a_2^1$	7.10 (0.90)	$...3e^34e^44a_1^21a_2^2$	4.97 (0.89)
			KO_4^-		
X	3.21 ± 0.08	$...2e^43e^31b_1^11a_2^1$	3.18 (0.93)	$...3e^44e^44a_1^21a_2^1$	3.05 (0.90)
A	4.1 ± 0.1	$...2e^43e^41b_1^11a_2^0$	4.46 (0.90)	$...3e^44e^44a_1^11a_2^2$	3.05 (0.90)
		$...2e^43e^41b_1^01a_2^1$	4.47 (0.90)	$...3e^44e^34a_1^21a_2^2$	3.94 (0.90)
		$...2e^33e^41b_1^11a_2^1$	7.04 (0.93)	$...3e^34e^44a_1^21a_2^2$	4.73 (0.90)

[a] All energies are in eV [b] Configurations with three unpaired electrons are all quartet states. [c] Pole strength is given in parentheses.

Table 9. Calculated Electron Detachment Processes and Vertical Detachment Energies (VDE) for the C_{3v} ($^1A_1$) and C_{2v} ($^3A_2$) Structures of NaO_5^- As Compared with the Experimental VDE

anion peak	exptl VDE (eV)	final state[a]	theory[b] VDE(eV) OVGF/6-311+G(2df)
		NaO_5^- (C_{3v}, $^1A_1$)	
X	3.53 ± 0.08	$...3e^45a_1^24e^45e^41a_2^1$	4.09 (0.87)
A	4.55 ± 0.06	$...3e^45a_1^24e^45e^31a_2^2$	4.64 (0.87)
		$...3e^45a_1^24e^35e^41a_2^2$	4.73 (0.91)
B	5.75 ± 0.04	$...3e^45a_1^14e^45e^41a_2^2$	5.89 (0.88)
C	6.15 ± 0.10	$...3e^35a_1^24e^45e^41a_2^2$	5.90 (0.87)
		NaO_5^- (C_{2v}, $^3B_2$)	
X	3.53 ± 0.08	$...6a_1^25b_1^21a_2^23b_2^12a_2^14b_2^1$	3.41 (0.93)
		$...6a_1^25b_1^21a_2^23b_2^22a_2^14b_2^0$	3.99 (0.92)
A	4.55 ± 0.06	$...6a_1^25b_1^21a_2^23b_2^22a_2^04b_2^1$	4.65 (0.90)
B	5.75 ± 0.04	$...6a_1^25b_1^21a_2^13b_2^22a_2^14b_2^1$	5.67 (0.92)
C	6.15 ± 0.10	$...6a_1^25b_1^11a_2^23b_2^22a_2^14b_2^1$	6.29 (0.92)
		$...6a_1^15b_1^21a_2^23b_2^22a_2^14b_2^1$	6.42 (0.92)

[a] Configurations with three unpaired electrons are all quartet states. [b] Pole strength is given in parentheses.

typical for dissociative detachment processes. Indeed, according to our calculations, the neutral $O_2^-M^+O_2$ cluster after the vertical electron detachment lies above the dissociation limit, $M^+O_2^- + O_2$, by 0.88, 0.71, and 0.68 eV for LiO_4, NaO_4, and KO_4, respectively. The values were calculated using the CCSD(T)/6-311+G(2df) energies of MO_4^-, MO_2, and O_2 and VDE of MO_4^- at UOVGF/6-311+G(2df). Therefore, both experimental and theoretical evidence indicates the observed MO_4^- species are actually of the $O_2^-M^+O_2^-$ form. The dissociative detachment processes imply that the PES spectra of MO_4^- would not yield the true ADEs because of the small Franck−Condon factors expected for the 0−0 transitions. Thus, the ADEs given in Table 1 should be viewed as the upper limits of the true values.

Photoelectron Spectra of NaO_5^-. We were also interested in confirming if the experimentally observed MO_5^- species, similar to the MO_4^- species, would contain a covalently bound O_5^{2-} dianion, analogous to SO_4^{2-}. The calculated photoelectron spectra of the anions with the C_{3v} and C_{2v} structures are compared with the experimental data in Table 9. Clearly, the calculated VDEs for the C_{2v} structure agrees better with the observed spectrum. The X band (Figure 3) was rather broad and should correspond to the first two detachment channels with calculated VDEs at 3.41 and 3.99 eV. Therefore, we believe that the experimentally observed NaO_5^- species was, indeed, of the form $O_2^-Na^+O_3^-$, consistent with energetics of the two isomers. According to the CCSD(T)/6-311+G(2df) calculations, the $O_2^-Na^+O_3^-$ isomer is more stable than the $Na^+O_5^{2-}$ isomer by 5.2 eV, even though the latter is a true minimum.

Conclusions

A combined experimental and theoretical effort was made to search for covalently bound higher oxygen species, O_4^{2-} and O_5^{2-}, analogous to the well-known inorganic anions, ClO_3^- and SO_3^{2-} and ClO_4^- and SO_4^{2-}, respectively. The experimental strategy was to stabilize the higher oxygen dianions in the forms of alkali complexes, $M^+O_4^{2-}$ and $M^+O_5^{2-}$. Indeed, strong mass signals were observed for MO_4^- and MO_5^- when alkali-atom-containing targets were laser-vaporized with an O_2-containing helium carrier gas. Photoelectron spectra were obtained for the MO_4^- and MO_5^- species and were compared with theoretical calculations. Our ab initio calculations showed that there exist two isomers for each MO_4^- and MO_5^- species. The ground states of the two anions are of the forms, $O_2^-M^+O_2^-$ and $O_2^-M^+O_3^-$, which are more stable than the covalently bound species, $M^+O_4^{2-}$ and $M^+O_5^{2-}$, respectively. Careful theoretical and experimental analyses revealed that the observed species were actually of the forms, $O_2^-M^+O_2^-$ and $O_2^-M^+O_3^-$ rather than the intended $M^+O_4^{2-}$ and $M^+O_5^{2-}$ species. However, the covalently bound forms are true minima on the potential energy surfaces, suggesting the viability for their potential syntheses under appropriate conditions. According to our ab initio calculations, the $M^+O_4^{2-}$ species were found to be just about 2.4−2.9 eV higher in energy than the $O_2^-M^+O_2^-$ species. It is interesting to note that the neutral covalently bound O_4 (an analogue of SO_3) was found to be 6.5 eV higher in energy than two separate O_2 molecules. Therefore, the tetra- and penta-atomic dianionic forms, O_4^{2-} and O_5^{2-}, might represent a more promising way to make the first covalently bound oxygen species with more than three oxygen atoms. Furthermore, in the solid state, some additional stability may derive from the Madelung force, which is absent in the gaseous anions.

Acknowledgment. The theoretical work was done at Utah State University and supported by a new faculty grant. The experimental work done at Washington State was supported by

the National Science Foundation (CHE-9817811) and performed at the W. R. Wiley Environmental Molecular Sciences Laboratory, a national scientific user facility sponsored by DOE's Office of Biological and Environmental Research and located at Pacific Northwest National Laboratory, which is operated for DOE by Battelle under Contract DE-AC06-76RLO 1830.

JA020097K